UNIVERSITY COLLEGE UTRECHT

Impurity States in Chern Insulators

by

Bram Boomsma (3991989)
Under the supervision of Dr. Lars Fritz
Research Thesis (UCSCIRES32)

30 June 2015

Abstract

This thesis examines in what ways the introduction of an impurity in an insulator (with and without topological order) affects the manifestation of in-gap bound states. This is done by constructing a model for the Chern insulator, adding an impurity in the form of a chemical potential, and studying how this alters the behavior of the system's electrons. Although this has been investigated analytically earlier this year [1], numerical evidence was not yet available. The results of this research show that in the topological insulator an additional in-gap bound state around the impurity emerges. Meanwhile, in-gap bound states remain generically absent in the case of the trivial insulator. This confirms the predictions of [1].

Acknowledgements

I would like to express my sincere gratitude to my supervisor Dr. Lars Fritz, for taking the time to help me become familiar with the material and answer any question I had.

Contents

Introduction

The theory of band structures is one of the pinnacles of contemporary condensed matter physics. Many properties witnessed in objects in the macroscopic world can be explained by appealing to the theory's description of the energy distribution of the matter's electrons in the microscopic world. For example, materials can be classified as conductors, semiconductors or insulators, depending on the magnitude of an energy gap between bands. If there is no gap between the highest occupied and the lowest unoccupied states, then the material is a conductor; if there is a gap between the two states, then the material is an insulator; semiconductors are insulators with smaller gaps, so that a small fraction of the electrons are able to bridge the gap. [2]

Recently, a new type of categorization has emerged, where materials are classified based on their topological order. This investigation of the topological order of materials has spawned the class of *topological insulators*; materials where the edges conduct (i.e., electrons are able to move along the edges) while the rest insulates. The aim of this thesis is to investigate in what ways an impurity affects the occurrence of in-gap bound states in insulators with and without topological order. [2, 3] The predictions of [1] will be verified for the Chern insulator.

In chapters 1 and 2 brief introductions to the relevant concepts of band theory and topological insulators respectively will be given. In chapter 3 the Chern insulator with and without impurity will be thoroughly examined and discussed. Chapter 4 concludes this research.

Chapter 1

Introduction to Band Theory

This chapter introduces the concepts of band theory relevant to the topic of this thesis. First Bloch's theorem will be given and explained, then a few exercises involving the tight-binding method will be done in order to get more familiar with the method, and the chapter will close with a discussion on closed versus open boundaries.

1.1 Bloch's Theorem

In a system with a periodic potential, such as electrons on a lattice, the Hamiltonian displays the translation invariance

$$H(\mathbf{r}) = H(\mathbf{r} + \mathbf{R}), \tag{1.1}$$

where $\mathbf{R}$ is a translation vector of the lattice. In other words, moving over to the next lattice point does not change the Hamiltonian. Bloch's theorem states that the eigenfunctions

$$\psi_{n,\mathbf{k}}(\mathbf{r}) = \mathrm{e}^{i\mathbf{k}\cdot\mathbf{r}} u_{n,\mathbf{k}}(\mathbf{r}),$$

where $\mathbf{k}$ is the wave vector (which takes values in the first Brillouin-zone), n is the band index and $u_{n,\mathbf{k}}(\mathbf{r})$ are periodic functions with the periodicity of the lattice, form a basis of solutions to the time-independent Schrödinger equation associated with equation 1.1. Since the wave vector $\mathbf{k}$ can have any value within the first Brillouin zone, there exists a continuous spectrum of energy eigenvalues for each $\psi_{n,\mathbf{k}}(\mathbf{r})$. [3, 4]

1.2 The Tight-Binding Method (Without Magnetic Field)

The tight-binding model is an approximation for when the wave functions of the atoms in a lattice overlap sufficiently so that adjustments to one's description of isolated atoms have to be made, but at the same time does not require one to abandon the description completely. This approximation permits one to easily find the band structure of the lattice. Consider a one-dimensional lattice (i.e. a chain) of N fixed lattice sites with bound electrons, with lattice constant a (see figure 1.1). The hopping parameter t expresses to what extent the wave function of an electron overlaps with the wave function of an electron at an adjacent lattice site. For $t = 0$, the electron is completely bound to the lattice site, and is unable to *hop* to another point, and for $t > 0$ hopping between lattice sites is possible. [4, 5] The Hamiltonian of this system is given by equation 1.2

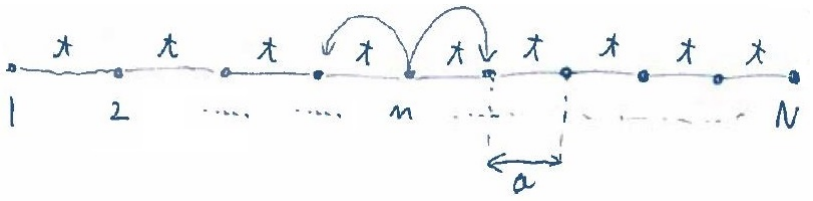

FIGURE 1.1: A one-dimensional lattice (i.e. a chain) with periodic boundaries.

$$H = -t\sum_{n=1}^{N}\left(c_n^\dagger c_{n+1} + c_{n+1}^\dagger c_n\right) - \mu\sum_{n=1}^{N} c_n^\dagger c_n, \tag{1.2}$$

where μ is the chemical potential. The operators $c_n^\dagger$ and c_n are fermionic raising/creation and lowering/annihilation operators respectively. These operators adhere to the following anti-commutation relations:

$$\left\{c_n, c_{n'}^\dagger\right\} = \delta_{n,n'},$$
$$\{c_n, c_n\} = \left\{c_n^\dagger, c_n^\dagger\right\} = 0,$$

and for a system consisting of unoccupied states $|0\rangle$ and occupied states $|1\rangle$:

$$c_n^\dagger|0\rangle = |1\rangle,$$
$$c_n^\dagger|1\rangle = 0,$$
$$c_n|1\rangle = |0\rangle,$$
$$c_n|0\rangle = 0.$$

According to the Pauli exclusion principle a single state of a system cannot be occupied by multiple electrons. Hence if the $c_n^\dagger$ operator is applied to an already occupied state

$|1\rangle$, 0 is returned. If the system is periodic, Fourier transformations can be performed on these operators:

$$c_n = \frac{1}{\sqrt{N}} \sum_k c_k \mathrm{e}^{-ikan},$$
$$c_n^\dagger = \frac{1}{\sqrt{N}} \sum_k c_k^\dagger \mathrm{e}^{ikan},$$

where $k = \frac{2\pi}{Na} m$ with $m \in [0, (Na) - 1]$. Using these relations, an expression for the Hamiltonian in equation 1.2 can be found in terms of the wave vector k in momentum space:

$$H = \sum_k c_k^\dagger c_k (-2t \cos ka - \mu).$$

Hence the energy dispersion is $\epsilon_k = -2t \cos ka - \mu$. [4]

Next, consider square lattices. A square lattice can be viewed as a number of chains with an equal number of lattice sites on top of each other. Let the hopping parameter t be the same in both the x-direction and the y-direction. Then the Hamiltonian for this system will be

$$H = -t \sum_{\mathbf{R}} \left(c_{\mathbf{R}+a\hat{\mathbf{x}}}^\dagger c_{\mathbf{R}} + c_{\mathbf{R}}^\dagger c_{\mathbf{R}+a\hat{\mathbf{x}}} + c_{\mathbf{R}+a\hat{\mathbf{y}}}^\dagger c_{\mathbf{R}} + c_{\mathbf{R}}^\dagger c_{\mathbf{R}+a\hat{\mathbf{y}}} \right) - \mu \sum_{\mathbf{R}} c_{\mathbf{R}}^\dagger c_{\mathbf{R}}. \tag{1.3}$$

Periodic boundaries allows for Fourier transforms, like before (with $n \to \mathbf{R}$ and $k \to \mathbf{k}$), to find the similar-looking Hamiltonian:

$$H = \sum_{\mathbf{k}} c_{\mathbf{k}}^\dagger c_{\mathbf{k}} (-2t(\cos(k_x a) + \cos(k_y a)) - \mu).$$

The energy dispersion is $\epsilon = -2t(\cos k_x a + \cos k_y a) - \mu$ (see figure 1.2). [4]

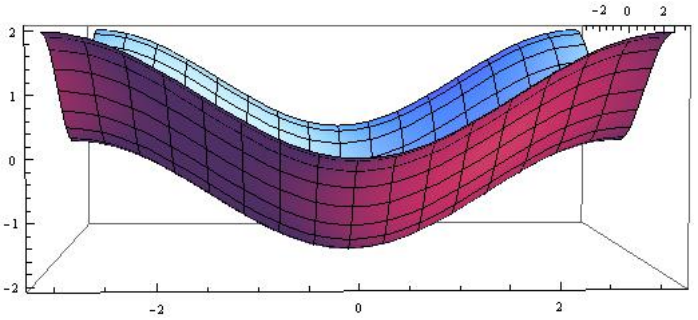

FIGURE 1.2: The band structure for the two-dimensional tight-binding chain with periodic boundary conditions.

If the lattice has open boundaries in both directions, the Hamiltonian can be written as

$$H = \begin{pmatrix} c_{1,1}^\dagger & c_{2,1}^\dagger & \cdots & c_{N,1}^\dagger & c_{1,2}^\dagger & \cdots & c_{N,N}^\dagger \end{pmatrix} \mathcal{H} \begin{pmatrix} c_{1,1} \\ c_{2,1} \\ \vdots \\ c_{N,1} \\ c_{1,2} \\ \vdots \\ c_{N,N} \end{pmatrix},$$

where

$$\mathcal{H} = I_N \otimes \begin{pmatrix} -\mu & -t & & & \\ -t & -\mu & -t & & \\ & -t & -\mu & \ddots & \\ & & \ddots & \ddots & -t \\ & & & -t & -\mu \end{pmatrix} + \begin{pmatrix} -\mu & -t & & & \\ -t & -\mu & -t & & \\ & -t & -\mu & \ddots & \\ & & \ddots & \ddots & -t \\ & & & -t & -\mu \end{pmatrix} \otimes I_N.$$

Figure 1.3 shows the energy eigenvalues of each site of a six-by-six lattice with open boundaries in both directions and no chemical potentials. Note that the distribution of the energy eigenvalues closely resembles the band structure found when assuming periodic boundary conditions.

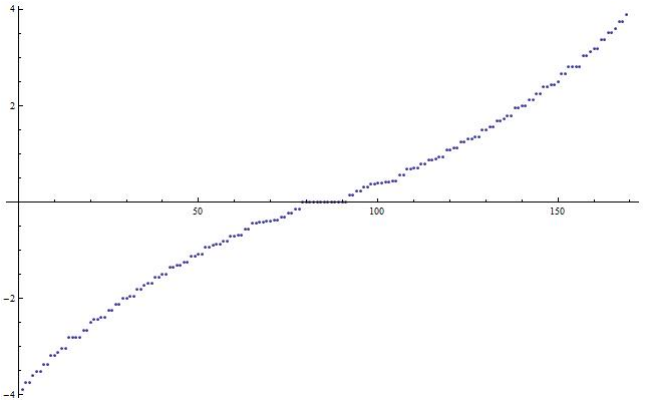

FIGURE 1.3: The energy eigenvalues of each site of a 13-by-13 lattice, sorted from lowest to highest, with open boundaries in both directions and no chemical potentials.

1.3 The Tight-Binding Method (With Magnetic Field)

Finally, the tight-binding method will be used to find the energy distribution of electrons on a square lattice subject to a magnetic field. The phase change the electrons pick up

by moving in closed surfaces due to the magnetic fluxes is

$$\begin{aligned}\phi &= \frac{e}{c\hbar}\int_a^b \mathbf{A}\cdot \mathrm{d}\mathbf{s} \\ &= \frac{e}{c\hbar}\int_a^b B\,\mathrm{d}S \\ &= \frac{2\pi\Phi}{\Phi_0}\end{aligned}$$

where $\Phi_0 \equiv \frac{c\hbar}{e}$. Hence the hopping parameter changes accordingly:

$$t \to t_{ab} = t\mathrm{e}^{i\phi} = t\mathrm{e}^{i\frac{2\pi\Phi}{\Phi_0}}$$

Let the lattice points be described as $(x, y) = (ma, na)$, and let the Landau gauge $\mathbf{A} = (0, Bx)$ be adopted. Then the hopping parameter in the x-direction is $t_n = t$ and in the y-direction $t_n = t\mathrm{e}^{i\frac{2\pi\Phi n}{\Phi_0}}$. From equation 1.3, the Hamiltonian will be

$$\begin{aligned}H =& -t\sum_{\mathbf{R}}\left(\mathrm{e}^{i\frac{2\pi\Phi}{a\Phi_0}\mathbf{R}\cdot\hat{\mathbf{x}}}c^\dagger_{\mathbf{R}+a\hat{\mathbf{y}}}c_{\mathbf{R}} + \mathrm{e}^{-i\frac{2\pi\Phi}{a\Phi_0}\mathbf{R}\cdot\hat{\mathbf{x}}}c^\dagger_{\mathbf{R}}c_{\mathbf{R}+a\hat{\mathbf{y}}} + c^\dagger_{\mathbf{R}+a\hat{\mathbf{x}}}c_{\mathbf{R}} + c^\dagger_{\mathbf{R}}c_{\mathbf{R}+a\hat{\mathbf{x}}}\right) \\ &- \mu\sum_{\mathbf{R}} c^\dagger_{\mathbf{R}}c_{\mathbf{R}}.\end{aligned}$$

In order to return translational invariance in the x-direction to the system, a new magnetic unit cell must be defined. A simple solution is to let $\frac{\Phi}{\Phi_0}$ be a rational number. Then, if an electron hops around the unit cell, it will pick up the phase $\mathrm{e}^{i2\pi j} = 1$, where j is an integer. For example, choose $\frac{\Phi}{\Phi_0} = \frac{1}{2}$ (and $a = t = 1$, $\mu = 0$). If an electron hops to the right once, up once, left once and then down once to arrive back at the starting position, the electron will have picked up a phase of $\mathrm{e}^{i\pi}$. However, if the electron hops to the right twice, up once, left twice and down once, it will have picked up the phase $\mathrm{e}^{i2\pi} = 1$. Hence, using this new magnetic unit cell, the unit vector in the x-direction (i.e. the horizontal direction) changes to $\hat{\mathbf{e}}_\mathbf{1} = 2\hat{\mathbf{x}}$, and consequently the Hamiltonian becomes

$$\begin{aligned}H = -t\sum_{\mathbf{R}}\Bigg[&\begin{pmatrix}A^\dagger_{\mathbf{R}} & B^\dagger_{\mathbf{R}}\end{pmatrix}\begin{pmatrix}0 & 1\\ 1 & 0\end{pmatrix}\begin{pmatrix}A_{\mathbf{R}}\\ B_{\mathbf{R}}\end{pmatrix} + \begin{pmatrix}A^\dagger_{\mathbf{R}+\hat{\mathbf{e}}_\mathbf{1}} & B^\dagger_{\mathbf{R}+\hat{\mathbf{e}}_\mathbf{1}}\end{pmatrix}\begin{pmatrix}0 & 1\\ 0 & 0\end{pmatrix}\begin{pmatrix}A_{\mathbf{R}}\\ B_{\mathbf{R}}\end{pmatrix} \\ &+ \begin{pmatrix}A^\dagger_{\mathbf{R}} & B^\dagger_{\mathbf{R}}\end{pmatrix}\begin{pmatrix}0 & 0\\ 1 & 0\end{pmatrix}\begin{pmatrix}A_{\mathbf{R}+\hat{\mathbf{e}}_\mathbf{1}}\\ B_{\mathbf{R}+\hat{\mathbf{e}}_\mathbf{1}}\end{pmatrix} + \begin{pmatrix}A^\dagger_{\mathbf{R}+\hat{\mathbf{e}}_\mathbf{2}} & B^\dagger_{\mathbf{R}+\hat{\mathbf{e}}_\mathbf{2}}\end{pmatrix}\begin{pmatrix}1 & 0\\ 0 & \mathrm{e}^{i\pi}\end{pmatrix}\begin{pmatrix}A_{\mathbf{R}}\\ B_{\mathbf{R}}\end{pmatrix} \\ &+ \begin{pmatrix}A^\dagger_{\mathbf{R}} & B^\dagger_{\mathbf{R}}\end{pmatrix}\begin{pmatrix}1 & 0\\ 0 & \mathrm{e}^{-i\pi}\end{pmatrix}\begin{pmatrix}A_{\mathbf{R}+\hat{\mathbf{e}}_\mathbf{2}}\\ B_{\mathbf{R}+\hat{\mathbf{e}}_\mathbf{2}}\end{pmatrix}\Bigg].\end{aligned}$$

Fourier transforming the Hamiltonian and adding the chemical potential yields

$$H = \sum_{\mathbf{k}} \begin{pmatrix} A_{\mathbf{k}}^\dagger & B_{\mathbf{k}}^\dagger \end{pmatrix} \begin{pmatrix} -te^{ik_y} - te^{-ik_y} - \mu & -t - te^{ik_x} \\ -t - te^{-ik_x} & -te^{i(k_y+\pi)} - te^{-i(k_y+\pi)} - \mu \end{pmatrix} \begin{pmatrix} A_{\mathbf{k}} \\ B_{\mathbf{k}} \end{pmatrix}$$
$$= \sum_{\mathbf{k}} \begin{pmatrix} A_{\mathbf{k}}^\dagger & B_{\mathbf{k}}^\dagger \end{pmatrix} \begin{pmatrix} -2t\cos k_y - \mu & -t - te^{ik_x} \\ -t - te^{-ik_x} & -2t\cos(k_y+\pi) - \mu \end{pmatrix} \begin{pmatrix} A_{\mathbf{k}} \\ B_{\mathbf{k}} \end{pmatrix}.$$

The band structure can be found by plotting the eigenvalues of the square matrix. [4]

In general the band structure for any value of $\frac{\Phi}{\Phi_0}$ can be found by finding the eigenvalues of the N-by-N matrix

$$\mathcal{H} = \begin{pmatrix} -f_0 - \mu & -t & 0 & \cdots & 0 & -te^{ik_x} \\ -t & -f_1 - \mu & -t & 0 & \cdots & 0 \\ 0 & -t & -f_2 - \mu & -t & 0 & \vdots \\ \vdots & & & \ddots & & 0 \\ 0 & & & & \ddots & -t \\ -te^{-ik_x} & 0 & & 0 & -t & -f_{N-1} - \mu \end{pmatrix}, \tag{1.4}$$

where $f_n = 2t\cos\left(k_y - 2\pi\frac{\Phi}{\Phi_0}n\right)$. [4]

Now, instead of having periodic boundaries in both the x-direction and y-direction, let the lattice have periodic boundaries in only the y-direction, while keeping the boundaries in the x-direction open. In this case Fourier transformations can only be performed on the y-direction, giving the square matrix:

$$\mathcal{H} = \begin{pmatrix} -f_0 - \mu & -t & & & & \\ -t & -f_1 - \mu & -t & & & \\ & -t & -f_2 - \mu & \ddots & & \\ & & \ddots & \ddots & -t & \\ & & & -t & -f_{N-1} - \mu \end{pmatrix}, \tag{1.5}$$

where f_n is the same as before. *Cutting open* the system is what causes the boundary modes to appear (see section 1.4 and figures 1.4 and 1.5).

1.4 Open Versus Closed Boundaries

The boundaries of a system determine its topology, its solutions, and the method of solving its Hamiltonian. A system with closed boundaries has periodic boundary conditions. The periodicity of the systems allow for Fourier transforms to be performed, making the

calculations relatively simple. Solving the Hamiltonian that way yields an energy distribution in terms of the wave vector $\mathbf{k}$. In the case of the chain the Hamiltonian is defined on a torus, and in the case of the square lattice it is defined on a sphere. Assuming a system has periodic boundaries is only valid when investigating the properties of the states in the center of the system. [3]

In the case of a square lattice where the system is periodic in only one direction, the Hamiltonian is defined on a cylinder. The system associated with equation 1.5 was periodic in only the y-direction, and therefore only the y-direction was Fourier transformed. The eigenvalues of equation 1.5 for $\frac{\Phi}{\Phi_0} = \frac{1}{3}$ and $\frac{\Phi}{\Phi_0} = \frac{1}{4}$ are plotted in the upper graphs of figures 1.4 and 1.5, for each value of k_y. Every line represents one lattice site in the y-direction, which when taken together create the band structure. [3]

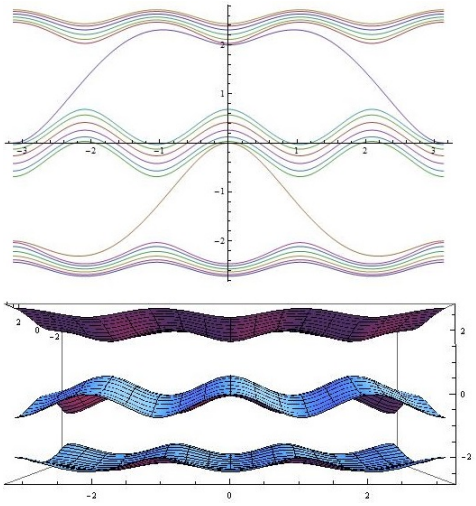

FIGURE 1.4: The band structure of the first Brillouin zone for $\frac{\Phi}{\Phi_0} = \frac{1}{3}$. The upper plot has closed boundaries in the y-direction, and the bottom plot has closed boundaries in both directions. In both plots $t = 1$ and $\mu = 0$, and in the upper plot the number of lattice sites is 20 and k_y is discretized with a step size of $\frac{\pi}{60}$.

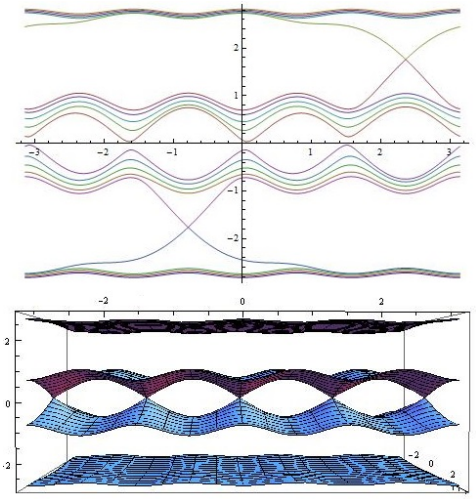

FIGURE 1.5: The band structure of the first Brillouin zone for $\frac{\Phi}{\Phi_0} = \frac{1}{4}$. The upper plot has closed boundaries in the y-direction, and the bottom plot has closed boundaries in both directions. In both plots $t = 1$ and $\mu = 0$, and in the upper plot the number of lattice sites is 20 and k_y is discretized with a step size of $\frac{\pi}{60}$.

The two plots in figure 1.4 look very similar to each other, as do the plots in figure 1.5. There are two differences between the plots. Firstly, the bands in the upper plots consist of a finite number of curves, whereas the bands in the lower plots are made up of continuous functions. These are *finite size effects*, and are not of great importance. Secondly, in the upper plots there are curves connecting the bands, while in the lower plots these are absent. These modes are known as *boundary modes*. Boundary modes live on the boundary of a system, and therefore they only appear in systems with (open) boundaries. The presence of these additional modes is proof that these systems are topological insulators, as will be elaborated on in section 2.1. [3]

Chapter 2

Topological Insulators

This chapter focuses on the topological insulator. First a short introduction to topology will be given, in order to become familiar with the concept of topological invariants and topological insulators. Then, to illustrate important properties of topological insulators, an example of a system with topological order will be considered: the quantum Hall system.

2.1 Introduction to Topology

The concepts of topological invariants and insulators can be understood more intuitively by studying topology in the context of mathematics. What do an orange and a glass have in common? And what do a donut and a mug have in common? The answer to both questions is *its topology*. The shapes of an orange and a glass can be transformed into one another through continuous deformations, and the same holds for the shapes of a donut and a mug. However, the shapes of oranges and glasses cannot be transformed into those of donuts and mugs that way, because they are topologically different. No continuous deformation of space can replicate the hole donuts and mugs have onto oranges and glasses. In this example the topological invariant is the number of holes in the object. [2]

One could categorize materials topologically according to whether or not there is an energy gap in the material's band structure. If the band structure of an insulator or a semiconductor can be transformed into the band structure of another material in the same category by changing the material's parameters continuously while maintaining an energy gap, then these two materials share the same topology (similar to how a torus and a mug do). Topological insulators are materials where the topological invariants are

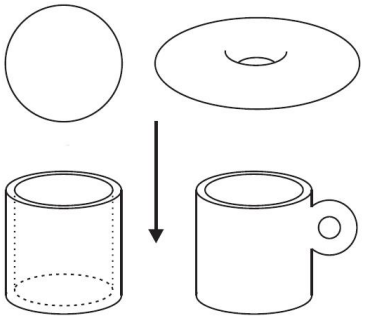

FIGURE 2.1: Through continuous deformations of space, a sphere can be transformed into a glass and a torus into a mug, or the other way around. [2]

not affected by continuous deformations, and whose band structures cannot transform in those of (trivial) insulators. Hence the band structures of topological insulators are topologically distinct from those of (trivial) insulators. [2]

Alternatively, topological insulators can be identified based on their response to changes in boundary conditions. Take a system with closed boundaries, and replace them with open boundaries. If additional modes emerge between the bands (as occurred in the upper plots of figures 1.4 and 1.5), then the system is a topological insulator. If no additional modes emerge, then the system is a (trivial) insulator. On a macroscopic level topological insulators can be identified for a conductor on the edges while being an insulator elsewhere. [2, 3]

2.2 The Quantum Hall Effect

The oldest system with topological order is the quantum Hall system. Originally, the Hall effect is the manifestation of a voltage difference in a two-dimensional conductor, subject to a perpendicular magnetic field and with an electric current running through it, transverse to the magnet field and the current. The Lorentz force due to the magnetic field bends the trajectory of the electrons in the conducting material, thereby causing negatively charged particles to go to one edge of the conductor, and positively charged particles to the opposite edge. In the classical limit, this so-called Hall voltage varies linearly with the strength of the magnetic field, and therefore, by Ohm's law, so does the transverse resistance. [4, 6–8]

However, this relation no longer holds in the limit of low temperatures and high magnetic fields, as was discovered by von Klitzing et al. in 1980. In this quantum mechanical limit the Hall resistance shows behavior of quantization: plateaus occur at certain values of the magnetic field, where the resistance on this plateaus is an integer or fractional

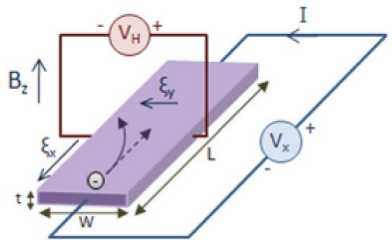

FIGURE 2.2: Experimental setup for measuring the Hall effect. [7]

multiple of fundamental constants, due to boundary modes in the system. Moreover, at these plateaus the longitudinal resistance disappears. [4, 6–8]

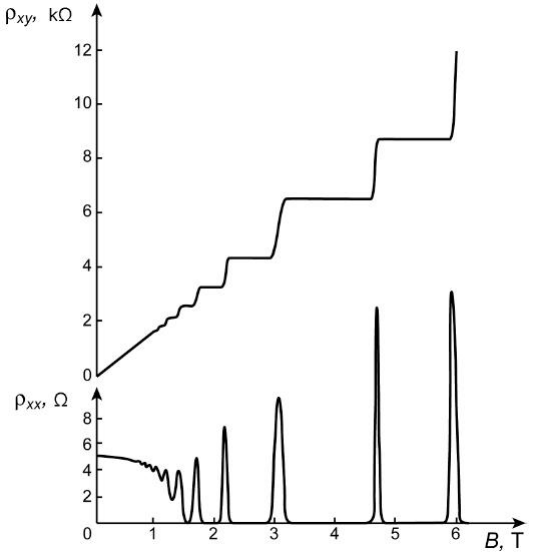

FIGURE 2.3: The Hall resistance and the longitudinal resistance versus the magnetic field and the temperature. At low values of B and T (i.e. the classical limit) the Hall resistance scales linearly with the magnetic field, while at higher values (the quantum limit) plateaus occur. At each plateau the longitudinal resistance disappears. [6]

A Bloch wave function $u_{n,\mathbf{k}}(\mathbf{r})$ picks up a phase ϕ when the wave vector $\mathbf{k}$ moves around in the BZ. The *Chern number* is defined as

$$n \equiv \sum \frac{1}{2\pi} \int \boldsymbol{\nabla} \times \phi \, \mathrm{d}^2\mathbf{k},$$

where the limits of integration cover the entire BZ, and the sum is over all occupied bands. This parameter denotes the number of Landau levels[1] $\epsilon_n = \hbar\omega_c\left(n + \frac{1}{2}\right)$ that are occupied, and has also been proved to be equal to the quantization constant in the equation for the Hall conductivity (which is the inverse of the Hall resistance):

$$\sigma = n\frac{e^2}{h}.$$

[1] See Appendix A.

The Chern number is what defines the topological order of the quantum Hall system. If the ground states of two distinct Hamiltonians have different Chern numbers, then that means they cannot be continuously deformed into one another, and thus that the systems associated with the Hamiltonians are not topologically identical. The fact that the Hall conductivity is determined by the Chern numbers is what gives it its topological structure. [6, 7]

Chapter 3

The Chern Insulator with Impurity

In this chapter the techniques and theory of the previous two chapters will be used to solve the Chern insulator. First the Chern insulator without impurity will be solved. Then an impurity in the form of a chemical potential will be added to the center of the system, and the results will be interpreted and linked to the predictions of [1].

3.1 The Chern Insulator Without Impurity

The Chern insulator is a caricature of the quantum Hall state: it is a lattice quantum Hall system without an external magnetic field. In this section the Hamiltonians for a lattice with closed boundaries in both directions and open boundaries in both directions will be solved. The electrons in this system will have two internal degrees of freedom, so the two-band model will be used to describe the Hamiltonian, since the hopping parameter is now given in terms of two-by-two matrices. Using the basis

$$I_2 = \begin{pmatrix} 1 & 0 \\ 0 & 1 \end{pmatrix}, \quad \sigma_x = \begin{pmatrix} 0 & 1 \\ 1 & 0 \end{pmatrix}, \quad \sigma_y = \begin{pmatrix} 0 & -i \\ i & 0 \end{pmatrix}, \quad \sigma_z = \begin{pmatrix} 1 & 0 \\ 0 & -1 \end{pmatrix}$$

the Hamiltonian of the Chern insulator can be written as

$$H = \sum_{\mathbf{R}} \Big[\Big(\frac{\sigma_z}{2} - \frac{\sigma_x}{2i} \Big) \Psi^\dagger_{\mathbf{R}} \Psi_{\mathbf{R}+x} + \Big(\frac{\sigma_z}{2} - \frac{\sigma_y}{2i} \Big) \Psi^\dagger_{\mathbf{R}} \Psi_{\mathbf{R}+y} + \text{h.c.} \Big] + m \sum_{\mathbf{R}} \sigma_z \Psi^\dagger_{\mathbf{R}} \Psi_{\mathbf{R}}, \quad (3.1)$$

where m is a mass parameter. [3, 6]

First consider the lattice with closed boundaries in both directions. As before, the Hamiltonian can be solved by performing Fourier transformations. Equation 3.1 then changes to

$$H = \sum_{k_x,k_y} \Psi^\dagger_{k_x,k_y}[(m + \cos(k_x) + \cos(k_y))\sigma_z + \sin(k_x)\sigma_x + \sin(k_y)\sigma_y]\Psi_{k_x,k_y}.$$

Hence there exists a $\vec{\mathbf{h}}(\mathbf{k})$ such that the kernel of the Hamiltonian can be expressed as

$$\mathcal{H}(\mathbf{k}) = \vec{\mathbf{h}}(\mathbf{k}) \cdot \vec{\sigma} = h_x\sigma_x + h_y\sigma_y + h_z\sigma_z,$$

with $\hat{\mathbf{h}}(\mathbf{k}) = \frac{\vec{\mathbf{h}}(\mathbf{k})}{|\vec{\mathbf{h}}(\mathbf{k})|}$. Then the Chern number n can be found by solving

$$n = \frac{1}{4\pi}\int_0^{2\pi} \mathrm{d}k_x\,\mathrm{d}k_y\,\hat{\mathbf{h}}(\mathbf{k}) \cdot \Big(\partial_x\hat{\mathbf{h}}(\mathbf{k}) \times \partial_y\hat{\mathbf{h}}(\mathbf{k})\Big).$$

The Chern number n is plotted against the mass parameter m in figure 3.1. The system

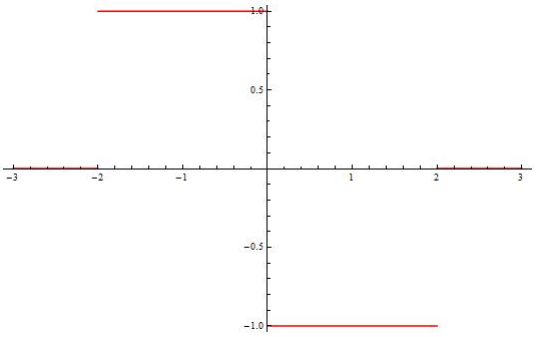

FIGURE 3.1: The Chern number n versus the mass parameter m. The system is a trivial insulator for $|m| > 2$, and a topological insulator elsewhere.

is a trivial insulator for $|m| > 2$, and a topological insulator elsewhere. Although there are different Chern Numbers associated with the systems where $m = \pm 0.1$, there are no visual difference between the bulk band structures (see figures 3.2 and 3.3). [3, 6]

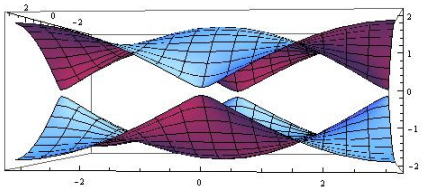

FIGURE 3.2: The spectrum of the Chern insulator obtained after diagonalizing the Hamiltonian of a system with periodic boundaries in both directions ($m = 0.1$).

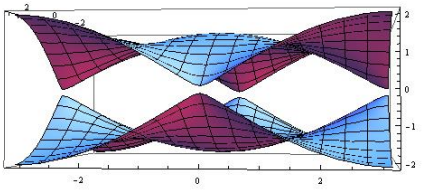

FIGURE 3.3: The spectrum of the Chern insulator obtained after diagonalizing the Hamiltonian of a system with periodic boundaries in both directions ($m = -0.1$).

Next consider the lattice with open boundaries in both directions. The kernel of this Hamiltonian[1] is

$$\mathcal{H} = I_N \otimes \mathcal{H}_1 + \begin{pmatrix} 0 & 1 & & & \\ 0 & 0 & 1 & & \\ & 0 & 0 & \ddots & \\ & & \ddots & \ddots & 1 \\ & & & 0 & 0 \end{pmatrix} \otimes \mathcal{H}_2 + \begin{pmatrix} 0 & 0 & & & \\ 1 & 0 & 0 & & \\ & 1 & 0 & \ddots & \\ & & \ddots & \ddots & 0 \\ & & & 1 & 0 \end{pmatrix} \otimes \mathcal{H}_2^{\mathsf{T}},$$

where

$$\mathcal{H}_1 = I_N \otimes m\sigma_z + \begin{pmatrix} 0 & 1 & & & \\ 0 & 0 & 1 & & \\ & 0 & 0 & \ddots & \\ & & \ddots & \ddots & 1 \\ & & & 0 & 0 \end{pmatrix} \otimes \left(\frac{\sigma_z + i\sigma_x}{2} \right) + \begin{pmatrix} 0 & 0 & & & \\ 1 & 0 & 0 & & \\ & 1 & 0 & \ddots & \\ & & \ddots & \ddots & 0 \\ & & & 1 & 0 \end{pmatrix} \otimes \left(\frac{\sigma_z - i\sigma_x}{2} \right)$$

$$\mathcal{H}_2 = I_N \otimes \left(\frac{\sigma_z - i\sigma_y}{2} \right).$$

For example, a two-by-two lattice would produce the matrix

$$\mathcal{H} = \begin{pmatrix} m & 0 & \frac{1}{2} & \frac{i}{2} & \frac{1}{2} & \frac{1}{2} & 0 & 0 \\ 0 & -m & \frac{i}{2} & -\frac{1}{2} & -\frac{1}{2} & -\frac{1}{2} & 0 & 0 \\ \frac{1}{2} & -\frac{i}{2} & m & 0 & 0 & 0 & \frac{1}{2} & \frac{1}{2} \\ -\frac{i}{2} & -\frac{1}{2} & 0 & -m & 0 & 0 & -\frac{1}{2} & -\frac{1}{2} \\ \frac{1}{2} & -\frac{1}{2} & 0 & 0 & m & 0 & \frac{1}{2} & \frac{i}{2} \\ \frac{1}{2} & -\frac{1}{2} & 0 & 0 & 0 & -m & \frac{i}{2} & -\frac{1}{2} \\ 0 & 0 & \frac{1}{2} & -\frac{1}{2} & \frac{1}{2} & -\frac{i}{2} & m & 0 \\ 0 & 0 & \frac{1}{2} & -\frac{1}{2} & -\frac{i}{2} & -\frac{1}{2} & 0 & -m \end{pmatrix}. \tag{3.2}$$

Since the Chern number changes when $m = 0$ and when $m = \pm 2$, this thesis will cover both cases $m = 1$ and $m = 3$. For $m = 1$ the system is a topological insulator (see

[1] Although this system's Hamiltonian is not Hermitian (since the kernel is not Hermitian, as equation 3.2 illustrates) it still produces real eigenvalues.

figure 3.4) and for $m = 3$ it is a trivial insulator (see figure 3.5), since there is a gap present.

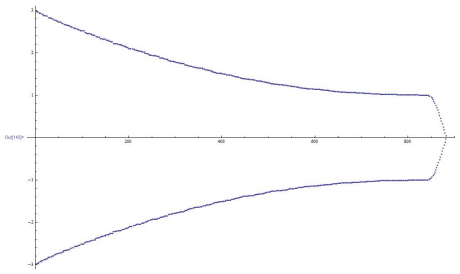

FIGURE 3.4: The energy spectrum of the Chern insulator for a 21-by-21 lattice ($m = 1$).

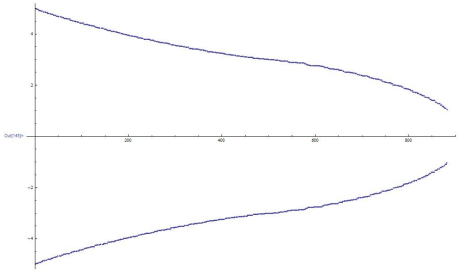

FIGURE 3.5: The energy spectrum of the Chern insulator for a 21-by-21 lattice ($m = 3$).

3.2 The Chern Insulator With Impurity

Now an impurity in the form of a chemical potential will be added to the lattice with open boundaries in both directions. To insert a chemical potential $-\mu$ to a lattice site (m, n) of an N-by-N lattice, $-\mu$ must be added to the entries $\left(N^2, N^2\right)$ and $\left(N^2+1, N^2+1\right)$ of the kernel of the Hamiltonian, since every lattice site is represented in the kernel as a two-by-two matrix. The energy spectra for the Chern insulator with an impurity in the center of the lattice are plotted in figures 3.6, 3.7, 3.8 and 3.9 for different values of m and μ. Note that there are two eigenvalues associated with every lattice site, since every lattice site is represented by a two-by-two matrix.

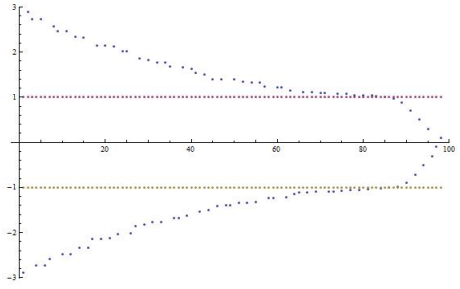

FIGURE 3.6: The energy spectrum of the Chern insulator **without impurity for a 7-by-7 lattice** ($m = 1$, $\mu = 0$)**. The horizontal lines at** ± 1 **indicate (approximately) the energy gap.**

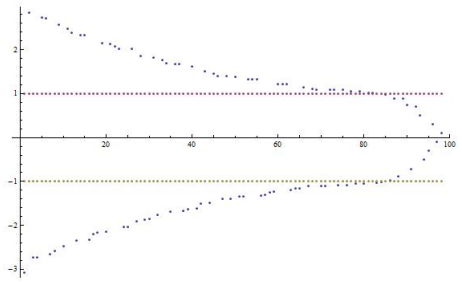

FIGURE 3.7: The energy spectrum of the Chern insulator **with impurity for a 7-by-7 lattice** ($m = 1$, $\mu = 1$)**. The horizontal lines at** ± 1 **indicate (approximately) the energy gap.**

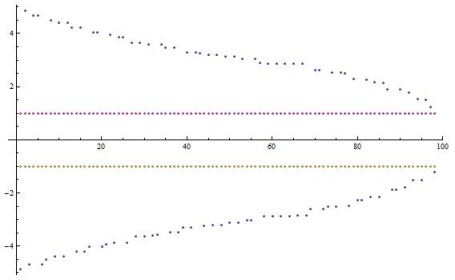

FIGURE 3.8: The energy spectrum of the Chern insulator **without impurity for a 7-by-7 lattice** ($m = 3$, $\mu = 0$)**. The horizontal lines at** ± 1 **indicate (approximately) the energy gap.**

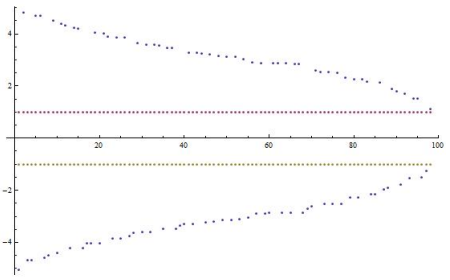

FIGURE 3.9: The energy spectrum of the Chern insulator **with impurity for a 7-by-7 lattice** ($m = 3$, $\mu = 1$)**. The horizontal lines at** ± 1 **indicate (approximately) the energy gap.**

3.2.1 Results for $m = 1$

There are no radical differences in the energy spectra between the systems of $\mu = 0$ and $\mu \neq 0$. Although individual energy eigenvalues change slightly, the energy spectrum retains its shape. However, the introduction of the impurity does cause two energy eigenvalues, which are associated with a single lattice site, to move from outside the energy gap to inside the gap (as can be seen in figure 3.6 (12 points in the gap) and figure 3.7 (14 points in the gap)). This phenomenon is not seen in systems with small lattices and small chemical potentials, due to finite-size effects. It is inconsequential if the chemical potential is positive or negative.

The additional eigenvalues in the gap represent *in-gap bound states*. In figure 3.10 the absolute value squared of the eigenvectors corresponding to the eigenvalues in the gap are plotted for a 17-by-17 lattice ($\mu = 1$). There is an additional plot associated with the smallest eigenvalue (absolute value) outside the defined[2] gap, to verify if the boundaries for the gap were approximated correctly. The plots show the probability wave function of the electrons for all the lattice sites. The numbers on the horizontal axis correspond to the lattice sites, counted horizontally. Note that the first plot does not show an electron that is bound, indicating that the size of the gap was not underestimated. The second plot is more ambiguous and one could claim that it shows an unbound electron, that therefore the gap was overestimated, and that hence the finding of the previous paragraph is not necessarily correct. However, if the same plots are created for the system without impurity (ceteris paribus), then the first three plots show clearly unbound electrons, while the fourth one is ambiguous. Hence the conclusion that the introduction of the impurity causes an extra lattice site to host bound electrons remains standing.

[2]The gap was estimated to consist of the eigenvalues between 1 and -1 (see for example figure 3.6 and figure 3.7).

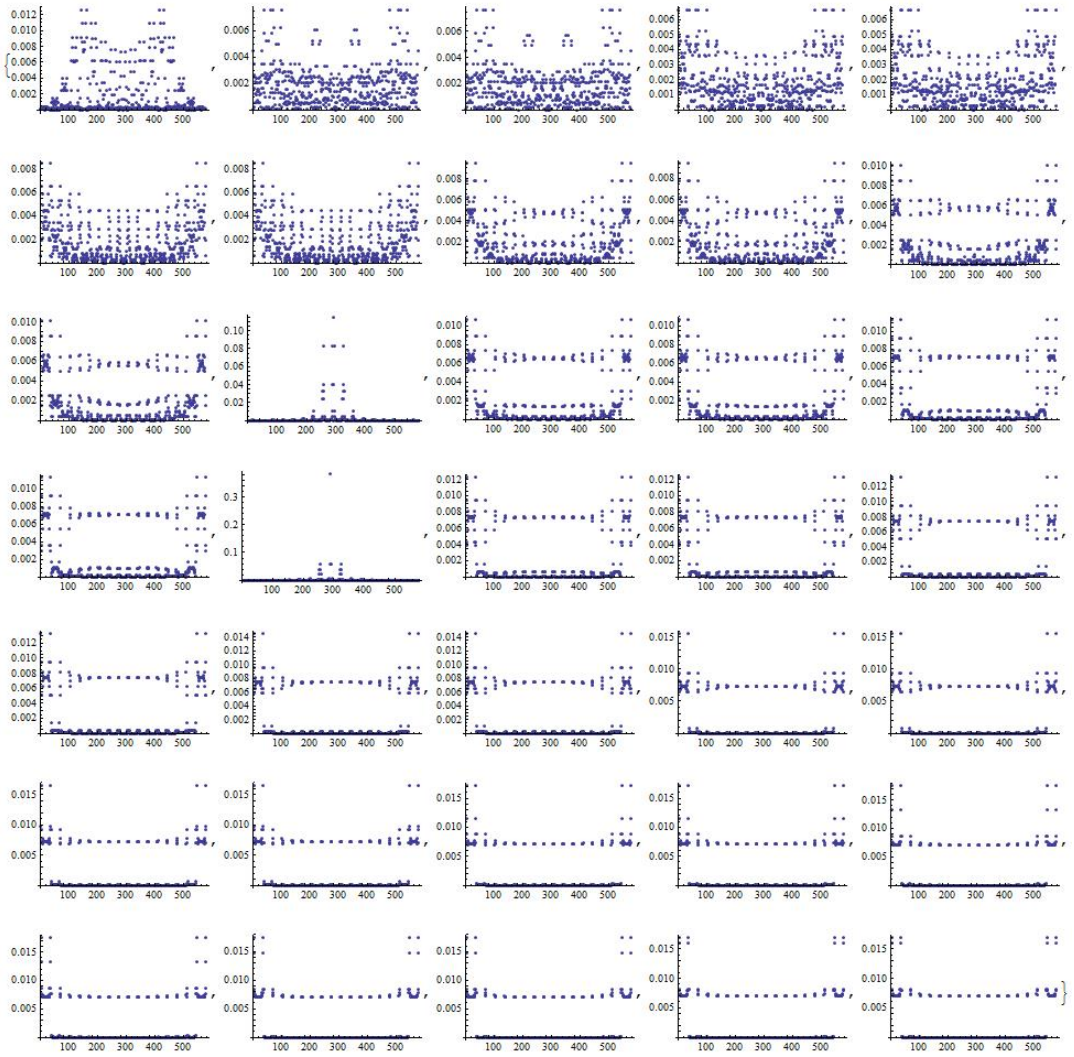

FIGURE 3.10: These plots show the probability (vertical axis) of electrons to be localized at specific lattice sites (horizontal axis, counted horizontally)) for all the bound electrons in a 17-by-17 lattice ($\mu = 1$). There is an additional plot to confirm the gap was well-defined.

The 12th and 17th plot (counted from left to right, top to bottom) have large peaks in the center, and are essentially zero elsewhere (see figure 3.11). Their maxima are at 289 and 290, which correspond to the lattice site where the chemical potential was introduced. Since no such plots appear in the system without impurity, it can be concluded that the additional bound state is localized around the impurity, as one would expect. The other plots represent the boundary modes (see figure 3.12). Since the lattice sites are counted horizontally, the first and last 17 numbers on the horizontal axis correspond to the top and bottom edges, while the left and right edges are represented by the 18th, 34th, 35th, 51st, 52nd, etc. numbers. These are exactly the numbers where the remaining plots show non-zero probabilities. Hence the bound states in the Chern insulator with an impurity are the boundary modes and the electrons in the chemical potential.

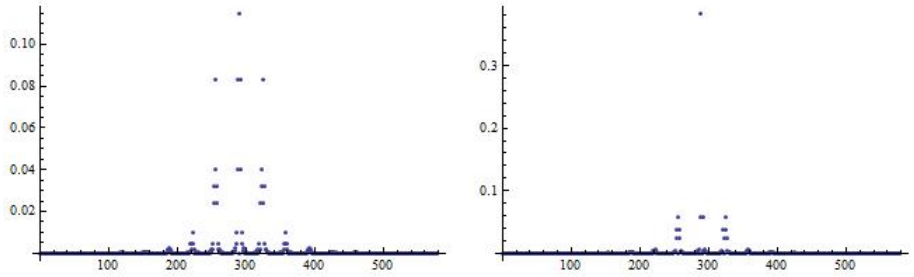

FIGURE 3.11: The 12th and 17th plot of figure 3.10. The maxima are at the numbers corresponding to the lattice site containing the impurity.

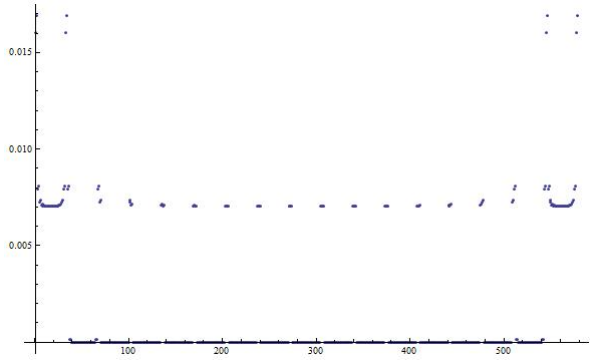

FIGURE 3.12: The last plot of figure 3.10. The other bound states of the system are at the edges, as is shown in this plot and the similar-looking plots in figure 3.10. Note that these boundary modes are also present when there is no impurity (ceteris paribus).

3.2.2 Results for $m = 3$

There are no radical differences in the energy spectra between the systems of $\mu = 0$ and $\mu \neq 0$. Although individual energy eigenvalues change slightly, the energy spectrum retains its shape. The impurity does not cause energy eigenvalues to appear inside the gap.

Chapter 4

Conclusion

In this thesis the effects an impurity, in the form of a chemical potential, has on the in-gap bound states of a Chern insulator are investigated. First, brief introductions to band theory and topology are provided in order to become more familiar with the topic and the method, and then a mathematical model representing the Chern insulator is created. This thesis concludes that for the topological insulator an additional bound state manifests itself, around the impurity, while bound states remain absent in the case of the trivial insulator. Further research could be performed to determine whether a change in the location of the impurity and/or the number of impurities radically alters the results.

Appendix A

Landau Levels

The Hamiltonian of an electron in a homogeneous magnetic field in two dimensions (ignoring electron spin) is

$$H = \frac{1}{2m}\boldsymbol{p}^2 = \frac{1}{2m}\Big(-i\hbar\boldsymbol{\nabla} - \frac{e}{c}\boldsymbol{A}\Big)^2.$$

This Hamiltonian can be solved in the same way the quantum harmonic oscillator is solved, using ladder operators:

$$a = \sqrt{\frac{c}{2\hbar eB}}(p_x - ip_y),$$

$$a^\dagger = \sqrt{\frac{c}{2\hbar eB}}(p_x + ip_y).$$

The new Hamiltonian is

$$H = \frac{\hbar eB}{mc}\left(a^\dagger a + \frac{1}{2}\right) \equiv \hbar\omega_c\left(a^\dagger a + \frac{1}{2}\right),$$

with energy eigenvalues

$$\epsilon_n = \hbar\omega_c\left(n + \frac{1}{2}\right).$$

These equidistant and degenerate energy levels are known as *Landau levels*. [4, 8]

Bibliography

[1] RJ. Slager, L. Rademaker, J. Zaanen, and L. Balents. Impurity Bound States and Greens Function Zeroes as Local Signatures of Topology. *arXiv preprint arXiv:1504.04881*, 2015. `http://arxiv.org/pdf/1504.04881.pdf`.

[2] M. H. Berntsen. *Consequences of a non-trivial band-structure topology in solids.* PhD thesis, Kungliga Tekniska högskolan, `http://www.diva-portal.org/smash/get/diva2:619836/FULLTEXT01.pdf`.

[3] B. de Leeuw. On the numerical computation of electron transport through a topological crystalline insulator. Master's thesis, Utrecht University.

[4] S. Matern. Hall-Leitfähigkeiten im Hofstadter-Schmetterling. Bachelor's thesis, Universität zu Köln.

[5] N. W. Ashcroft and N. D. Mermin. *Soid State Physics.* Holt, Rinehart and Winston, 1976. ISBN 0030839939.

[6] A. Altland and L. Fritz. Primer on topological insulators. Lecture notes.

[7] Ž. Kos. *Topological insulators.* Univerza v Ljubljani, 2013. `http://mafija.fmf.uni-lj.si/seminar/files/2012_2013/seminar1b_Ziga_Kos.pdf`.

[8] D. Yoshioka. *The Quantum Hall Effect.* Springer Series in Solid-State Sciences. Springer Berlin Heidelberg, 2002. ISBN 9783642077203.